### Title

New Architecture for Reagentless, Protein-Based Electrochemical Biosensors




### Journal

Journal of the American Chemical Society, 139(35)

### ISSN

0002-7863



### Authors

Kang, Di
Sun, Sheng
Kurnik, Martin
et al.



### Publication Date

2017-09-06

### DOI

10.1021/jacs.7b05953

Peer reviewed

Published in final edited form as:

*J Am Chem Soc*. 2017 September 06; 139(35): 12113–12116. doi:10.1021/jacs.7b05953.

# A new architecture for reagentless, protein-based electrochemical biosensors

**Di Kang**[1,+], **Sheng Sun**[1,+], **Martin Kurnik**[1], **Demosthenes Morales**[1], **Frederick W. Dahlquist**[1], and **Kevin W. Plaxco**[1,2]

[1]Department of Chemistry and Biochemistry, University of California, Santa Barbara, CA 93106 USA

[2]Interdepartmental Program in Biomolecular Science and Engineering, University of California, Santa Barbara, CA 93106 USA

## Abstract

Here we demonstrate a new class of reagentless, single-step sensors for monitoring protein-protein and protein-peptide interactions that is the electrochemical analog of fluorescence polarization (fluorescence anisotropy), a versatile optical approach widely employed to this same end. Our electrochemical sensors consist of a redox-reporter-modified protein (the "receptor") site-specifically anchored to an electrode via a short, flexible polypeptide linker. Interaction of the protein with its binding partner alters the efficiency with which the attached reporter approaches the electrode surface, thus changing the observed redox current upon voltammetric interrogation. As proof-of-principle we employed the bacterial chemotaxis protein CheY as our receptor. Interaction with either of CheY's two binding partners, the P2 domain of the chemotaxis kinase, CheA, or the 16-residue "target region" of the flagellar switch protein, FliM, leads to easily measurable changes in output current that trace Langmuir isotherms within error of those seen in solution. Phosphorylation of the electrode-bound CheY decreases its affinity for CheA-P2 and enhances its affinity for FliM in a manner likewise consistent with its behavior in solution. As expected given the proposed sensor signaling mechanism, the magnitude of the binding-induced signal change depends on the placement of the redox reporter on the protein. Following these preliminary studies with CheY we also developed and characterized additional sensors aimed at the detection of specific antibodies using the relevant protein antigens as the receptor. These exhibit excellent detection limits for their targets without the use of reagents or wash steps. This novel, protein-based electrochemical sensing architecture provides a new and potentially promising approach to quantitative, single-step detection of specific proteins and peptides.

## TOC image

**Corresponding Author:** kwp@chem.ucsb.edu.
[+]These authors contributed equally.

**Supporting Information**

The Supporting Information is available free of charge on the ACS Publications website. This includes methods and further data supporting the conclusions described here.

***Notes***

The authors declare no competing financial interests.

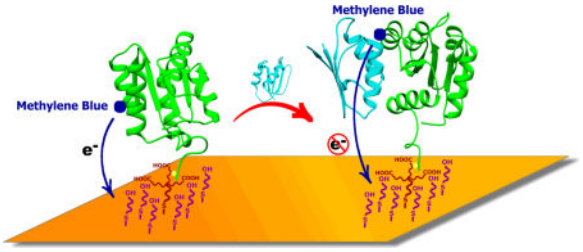


Among quantitative methods for measuring the levels of specific, diagnostically relevant proteins, only fluorescence polarization (also known as fluorescence anisotropy)[1] has seen wide use in point-of-care applications[2–6]. This approach, which reports on the presence of a specific protein-protein complex via binding-induced changes in the tumbling of an attached fluorophore, does not require washing to remove unbound reagents, rendering it one of the more convenient methods for quantifying the levels of specific proteins in clinical samples. Several limitations, however, significantly reduce its utility at the point of care. For example, when challenged with authentic clinical samples the approach requires considerable signal averaging and careful background subtraction. In part, this is due to its modest signal gain: the intensity difference between the two polarizations is typically of order ~15% (i.e., 150 millipolarization units) for an antibody-antigen complex, which must be measured against background polarizations of similar magnitude[7–9]. Fluorescence polarization also requires fairly large sample volumes, necessitating venous blood draws that further reduce its utility at the point of care. Finally, fluorescence polarization is not easily multiplexed, rendering it ill-suited for the simultaneous monitoring of, for example, multiple antibodies diagnostic of a single pathogen or simultaneously monitoring for antibodies against multiple pathogens.

In response to the above arguments a number of groups have developed electrochemistry-based sensing platforms that attempt to capture the generality of fluorescence polarization while avoiding some of its limitations[10–12]. In previous work, for example, we developed an electrochemical approach utilizing a double-stranded nucleic acid “scaffold” modified on one end to present both a protein-recognizing polypeptide or small molecule and a redox reporter and covalently attached to gold electrode via a flexible linker via the other[10,13–15]. The binding of the sensor’s target to this recognition element reduces the efficiency with which the attached redox reporter approaches the electrode (analogous to the change in tumbling seen in fluorescence polarization), producing an easily measured change in electron transfer efficiency (analogous to a change in fluorescence polarization). This strategy offers several potential advantages over other methods for detecting protein-polypeptide and protein-small-molecule interactions, including the reduced complexity associated with its reagentless, single-step, wash-free format and better performance in complex samples, such as undiluted blood serum and crude soil extracts[10]. Here we expand this approach by demonstrating sensors that, rather than using a double-stranded DNA scaffold and a relatively low molecular weight recognition element (e.g., a polypeptide), instead employ full-length proteins as both the recognition element (receptor) and the scaffold, expanding the range of analytes that the approach can be used to detect.

Here we demonstrate a single-step electrochemical approach for measuring specific protein-protein and protein-peptide interactions that should be expandable to a wide range of other macromolecular targets. As our first test bed, we employed as our receptor CheY, a response regulator protein from the *E. coli* chemotaxis signal transduction system. The structure and folding of CheY and its binding to its protein and peptide targets CheA-P2 and $FliM_{16}$ have seen extensive prior study[16–19], rendering them a convenient model system. To convert CheY into a single-step electrochemical sensor we first generated a family of CheY variants containing a carboxy-terminal hexa-His-tag with each exposing a single cysteine side chain for conjugation to a maleimide-functionalized methylene blue. To generate our sensors, we then used copper complexation with the His-tag to attach each modified protein onto a gold electrode coated with an alkane thiol self-assembled monolayer doped with a small fraction of copper chelating nitrilotriacetic acid (NTA) head groups (Figure 1a). We employed copper, rather than nickel, as histidine-copper complexes are less kinetically labile.

Our new sensor architecture responds quantitatively when challenged with the appropriate target molecule. In the absence of either of CheY's binding partners the redox reporter is relatively free to collide with the electrode surface, producing a large faradaic current at the redox potential expected for methylene blue when the system is interrogated using cyclic voltammetry (Figure 1a, left). This peak is reduced in the presence of the protein's binding partners (Figure 1a right). For example, for a CheY modified with the redox reporter at position 97, the current falls 22% upon the addition 100 μM of the ligand CheA-P2, a 74-residue protein that is part of the bacterial chemotaxis system, with a time constant of $2.8\pm0.7\ min^{-1}$ (Figure 1d). Upon titration, the observed signal change increases monotonically with increasing ligand concentration until it approaches saturation at a change of 24% (Figure 2b). The resultant binding curve is well fitted with a Langmuir isotherm, producing a dissociation constant of 14 ± 4 μM (Figure 2b), which is within error of the value previously reported for this interaction when the proteins are free in solution[20,21]. As expected for electrochemical sensors of this class, the sensor also performs well when challenged in complex sample matrices. For example, the sensor's gain is only slightly reduced, to 17% (reporter at position 97) when it is challenged in 20% blood serum (Figure SI 1).

The signal gain of this sensor (the relative signal change seen upon the addition of saturating target) depends on both the attachment-position of the methylene blue and the structure of the target. To illustrate the former, we fabricated seven sensors differing only in the residue on which the methylene blue was attached using the variants M17C, E37C, T71C, A80C, G89C, K91C, K97C and E117 (Figure 3). The signal gain observed for these when we employ CheA-P2 as the target range from 4% to 30% (Figure 3, Table SI 1), with the later value larger than the signal change typically seen in fluorescence polarization assays[9]. The largest gain is seen when the redox-reporter is placed closest to the CheA-binding site (position 97) (Figure 2b, d), suggesting that much of the signal change arises due to steric blocking of the redox reporter by the target protein. Consistent with this, the gain of the sensor is abated when the reporter is positioned farther from the binding site (e.g., at E37C or A80C). We also investigated the sensor's ability to detect a second naturally occurring binding CheY binding partner, the 16-residue peptide $FliM_{16}$, finding behavior similar to that observed for the detection of CheA-P2 (Figure 2a,c). Specifically, a sensor modified

with methylene blue near the binding site (at residue 91) exhibits the greatest gain (14%). The signal gain observed upon $FliM_{16}$ binding, however, is generally less than that observed upon CheA-P2 binding. We presume this occurs as a consequence of the larger bulk of CheA-P2, which would more easily hinder approach of the reporter to the electrode.

This new sensor architecture readily detects changes in binding affinity associated with the phosphorylation of CheY. Phosphorylation induces allosteric communication between the phosphorylation site (D57) and the target-binding site[18,22,23], which in turn facilitates CheY's dissociation from CheA while strengthening its interactions with the flagellar motor switch protein FliM. Consistent with this, we see significant decreases and increases in affinity for CheA-P2 and $FliM_{16}$, respectively, upon phosphorylation of the surface-bound CheY. Specifically, the phosphorylation of surface-bound CheY enhances its affinity for $FliM_{16}$ by a factor of ca. 15 (Figure 2c), which is consistent with the results of prior solution-phase studies[24,25] and what we have observed via tryptophan fluorescence quenching experiments in free solution (Figure SI 2, 3). The phosphoryation of surface-bound CheY likewise reduces its affinity for CheA-P2 by a factor of ca. 5 (Figure 2d). Finally, we introduced D57A mutation to our CheY single-cysteine variants, which disables the phosphorylation of CheY. Consistent with expectations, the affinity of this variant is not altered by the presence of the phosphorylating agent acetyl phosphate (Figure SI 4).

The successful use of CheY as a recognition element for the detection of CheA and FliM motivated us to explore the approach's ability to detect specific antibodies via the inclusion of the relevant antigen as the recognition element. To do so we first employed green fluorescent protein (GFP) modified with methylene blue at random lysine epsilon amino groups or cysteine thiols as a receptor for the detection of GFP-binding antibodies (Figure 4a). Using polyclonal anti-GFP antibodies as our target we observe Langmuir isotherm binding with a dissociation constant 53±8 ng/ml, which is the equivalent of ~0.3 nM for the mixed antibody concentration (Figure 4b). As a second test of our ability to detect specific antibodies we employed a disease-related, clinically relevant antigen-antibody pair, the hepatitis B surface antigen (HBsAg) and anti-hepatitis antibodies (HBsAb). Using HBsAg modified with methylene blue at random lysine epsilon amino groups or at cysteine thiols as our recognition element we can detect the antibody with a detection limit of a few nanograms per milliliter (Figure 4c), a value that compares well with commercial approaches[26]. A test of this sensor in 20% blood serum, reflecting more authentic clinical conditions, renders its detection limit effectively unchanged (Figure 4d).

Here we demonstrate a new class of reagentless, single-step sensors that is the electrochemical analog to optical fluorescence polarization assays. As proof of principle we have used the approach to monitor the interaction of CheY with its two binding partners, the P2 domain of CheA and the 16-residue peptide $FliM_{16}$ and for the detection of both anti-GFP and anti-HBsAg antibodies. In all cases, we observed binding induced signal changes as large or larger than those typically seen in fluorescence polarization[9] without the need for light sources, optics, or extensive signal averaging. This new protein-based, electrochemical sensing platform provides us an alternative means to fluorescence polarization for probing protein-macromolecular interactions and thus may be a promising tool for both scientific and clinical applications. Similar to fluorescence polarization, for example, our protein based

scaffold approach is single step and label-free, rendering it faster, and, likely, less costly ELISAs and western blots[27]. The approach also offers potential advantages over fluorescence polarization, including its relatively inexpensive supporting electronics[28], its ability to perform well in relatively high concentrations of blood serum (Figure 4 and Figure SI 1), and the ready multiplexing of electrochemical approaches[29,30].

## Supplementary Material

Refer to Web version on PubMed Central for supplementary material.

## Acknowledgments

The authors wish to thank Dr. Guoya Mo for helpful technical discussions. This work was supported by the NIH through grants R01AI107936 and R01GM59544.

## References

1. Dandliker WB, Kelly RJ, Dandliker J, Farquhar J, Levin J. Immunochemistry. 1973; 10:219. [PubMed: 4580370]
2. Melanson SEF. Point of Care. 2005; 4:123.
3. von Lode P. Clin Biochem. 2005; 38:591. [PubMed: 16009140]
4. Jameson DM, Ross JA. Chem Rev. 2010; 110:2685. [PubMed: 20232898]
5. Lea WA, Simeonov A. Expert Opin Drug Dis. 2011; 6:17.
6. Nguyen HH, Park J, Kang S, Kim M. Sensors-Basel. 2015; 15:10481. [PubMed: 25951336]
7. Nielsen K, Gall D. J Immunoass Immunoch. 2001; 22:183.
8. Lucero NE, Escobar GI, Ayala SM, Paulo PS, Nielsen K. J Med Microbiol. 2003; 52:883. [PubMed: 12972582]
9. Rossi AM, Taylor CW. Nat Protoc. 2011; 6:365. [PubMed: 21372817]
10. Cash KJ, Ricci F, Plaxco KW. J Am Chem Soc. 2009; 131:6955. [PubMed: 19413316]
11. Gerasimov JY, Lai RY. Chem Commun. 2010; 46:395.
12. McQuistan A, Zaitouna AJ, Echeverria E, Lai RY. Chem Commun. 2014; 50:4690.
13. Cash KJ, Ricci F, Plaxco KW. Chem Commun. 2009; 6222
14. White RJ, Kallewaard HM, Hsieh W, Adriana SPatterson AS, Jesse BKasehagen JB, Cash KJ, Uzawa T, Soh HT, Plaxco KW. Anal Chem. 2012; 84:1098. [PubMed: 22145706]
15. Bonham AJ, Paden NG, Ricci F, Plaxco KW. Analyst. 2013; 138:5580. [PubMed: 23905162]
16. Schuster M, Silversmith RE, Bourret RB. P Natl Acad Sci USA. 2001; 98:6003.
17. Baker MD, Wolanin PM, Stock JB. Bioessays. 2006; 28:9. [PubMed: 16369945]
18. Dyer CM, Dahlquist FW. J Bacteriol. 2006; 188:7354. [PubMed: 17050923]
19. Mo GY, Zhou HJ, Kawamura T, Dahlquist FW. Biochemistry. 2012; 51:3786. [PubMed: 22494339]
20. Li JY, Swanson RV, Simon MI, Weis RM. Biochemistry. 1995; 34:14626. [PubMed: 7578071]
21. Swanson RV, Lowry DF, Matsumura P, McEvoy MM, Simon MI, Dahlquist FW. Nat Struct Biol. 1995; 2:906. [PubMed: 7552716]
22. Appleby JL, Bourret RB. J Bacteriol. 1998; 180:3563. [PubMed: 9657998]
23. Zhao R, Collins EJ, Bourret RB, Silversmith RE. Nat Struct Mol Biol. 2002; 9:570.
24. Welch M, Oosawa K, Aizawa SI, Eisenbach M. P Natl Acad Sci USA. 1993; 90:8787.
25. Shukla D, Matsumura P. J Biol Chem. 1995; 270:24414. [PubMed: 7592655]
26. Tsai HY, Chan JR, Li YC, Cheng FC, Fuh CB. Biosens Bioelectron. 2010; 25:2701. [PubMed: 20494568]
27. Crowther, JR. The ELISA Guidebook. Humana Press Inc; 2001.

28. Rowe AA, Bonham AJ, White RJ, Zimmer MP, Yadgar RJ, Hobza TM, Honea JW, Ben-Yaacov I, Plaxco KW. Plos One. 2011; 6:e23783. [PubMed: 21931613]
29. Kang D, White RJ, Xia F, Zuo X, Vallée-Bélisle A, Plaxco KW. NPG Asia Mater. 2012; 4:e1.
30. Xia J, Song D, Wang Z, Zhang F, Yang M, Gui R, Xia L, Bi S, Xia Y, Li Y, Xia L. Biosens Bioelectron. 2015; 68:55. [PubMed: 25558873]

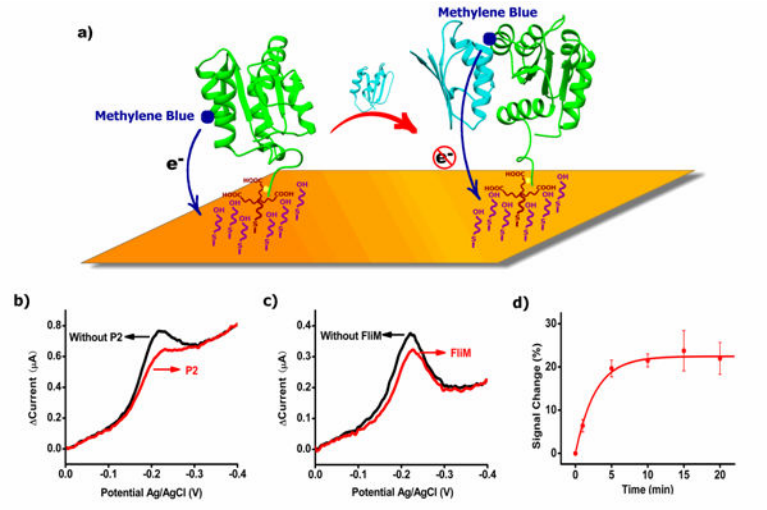


**Figure 1.**

Our sensor is comprised of a redox-reporter-modified protein that acts as a recognition element (receptor) attached to a gold electrode via a NTA-modified, thiol-on-gold self-assembled monolayer. a) Signal generation occurs when a target protein or peptide binds to this recognition element, reducing the efficiency with which the attached reporter (here methylene blue; shown as a blue dot) transfers electrons to the electrode. b) and c) This in turn, leads to an easily measured decrease in peak (faradaic) current; shown is the response of a sensor comprised of the bacterial chemotaxis protein CheY with a redox reporter at position 97 to CheY's naturally occurring binding partner CheA-P2 and a redox reporter at position 91 to $FliM_{16}$. d) The sensor response is rapid; when the CheY-presenting sensor is exposed to 100 μM of the target CheA-P2 it equilibrates with a time constant 2.8±0.7 $min^{-1}$. The error bars reflect standard deviations of independently fabricated sensors.

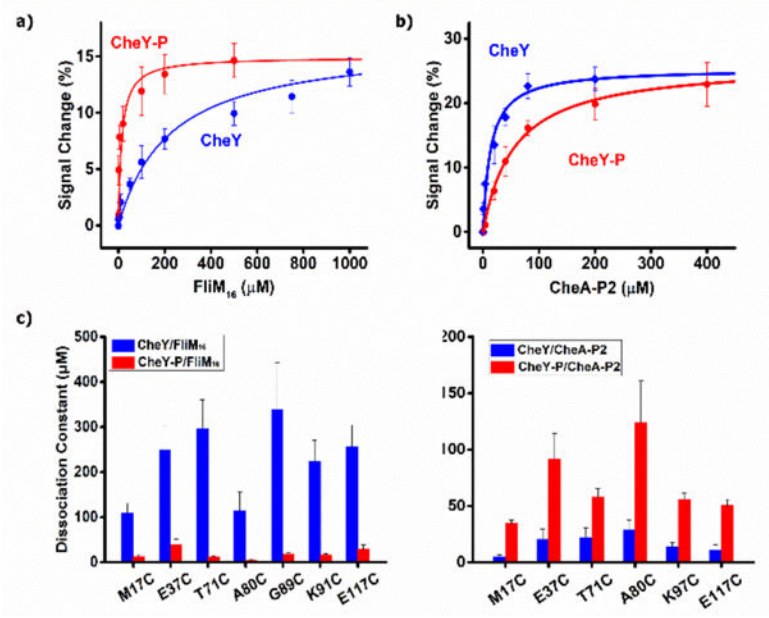


**Figure 2.**

As expected, the affinities with which surface-bound CheY bind$FliM_{16}$ and CheA-P2 change significantly upon phosphorylation. a) The dissociation constant for $FliM_{16}$ binding, for example, shifts from 213±48 03BCM to 16±3 μM upon phosphorylation (redox reporter at position 91). This ca. 15-fold change is consistent with the results of prior solution-phase studies[20,21]. b) The dissociation constant for CheA-P2 binding likewise shifts, albeit rising rather than falling (from 14±4 μM to 56±5 μM) upon phosphorylation (redox reporter at position 97). Similar changes are seen for all CheY labeled at other positions when challenged with c) $FliM_{16}$ or d) CheA-P2. The error bars here and elsewhere in this work reflect standard deviations of independently fabricated and measured sensors.

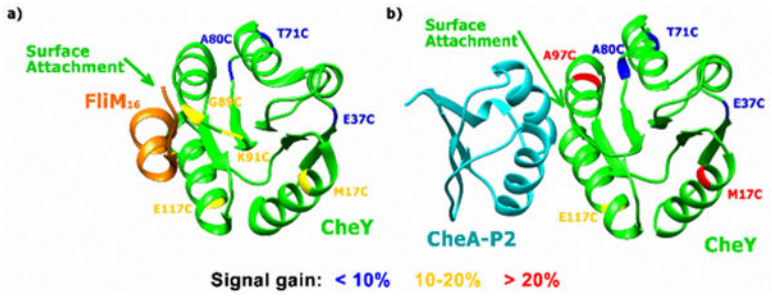


**Figure 3.**

Not surprisingly, signal gain in this class of sensors depends on the placement of the redox reporter relative to the target-binding and surface attachment sites with the greatest signal gain generally being observed when the reporter is positioned adjacent to the binding site. Non-green residues in this illustration reflect positions on CheY that we have modified with the methylene blue redox reporter. The coloring indicates the signal change seen for each variant upon ligand binding (<10% blue, 10-20% yellow, >20% red).

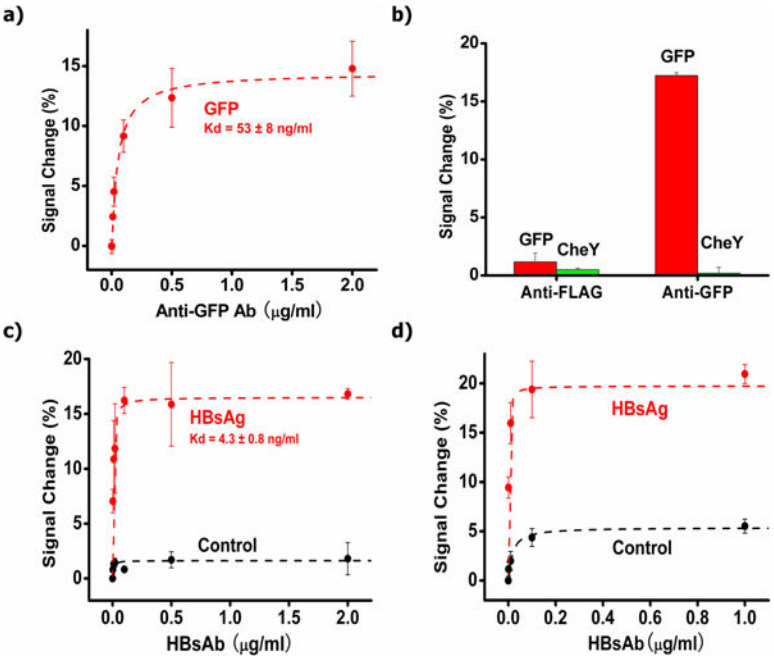


**Figure 4.**

Our sensing platform can also be used to monitor antigen-antibody interactions. a) For example, using an electrode-bound, redox-reporter-modified Green Fluorescent Protein (GFP) as the recognition element we easily detect anti-GFP antibodies at 10 ng/ml (the lowest concentration shown on this plot). The monotonic response obtained when the receptor is GFP modified with a methylene blue on random lysine residues. A similar curve is seen for the protein modified on random cysteine residues (Figure SI 5a). b) In contrast, the sensor does not produce respond to a negative control antibody (anti-FLAG) at 1 μg/ml. Likewise a sensor employing CheY does not produce any signal in response to either anti-Flag or anti-GFP antibodies at 1 μg/ml. c) Using a hepatitis B surface antigen (HBsAg) modified with methylene blue on random cysteines as the receptor we can similarly detect antibodies against this protein (HBsAb). We use CheY sensor as control for HBsAb binding. A similar curve is seen for the protein modified on random cysteine residues (Figure SI 5b). Shown are binding curves collected in buffer and, d) in 20% blood serum.